

https://dspace.org/

Evaluation of pipe stub flange behaviour during hydrostatic pressure testing

Asumani, Oscar

2008-05-16T07:19:21Z
http://hdl.handle.net/10539/4833

Downloaded from a DSpace repository. https://dspace.org/

APPENDIX A - INTERNATIONAL STANDARDS RELATING TO THE DESIGN, MANUFACTURING AND TESTING PROCEDURES OF FRP PIPE JOINTS

1. "2001 Boiler and pressure vessel code", ASME 10 CODES
2. "Standard specification for fibreglass pressure pipe fittings", ASTM D5685-95
3. "Standard specification for contact moulded fibreglass flanges", ASTM D5421-93
4. "Standard practice for determining dimensions of fibreglass pipes and fittings", ASTM D 3567-97
5. "Standard practice for selecting bolting lengths for piping system flanged joints", ASTM F704-81
6. "Standard test method for cyclic pressure strength of reinforced thermosetting plastic pipe", ASTM D2143-00
7. "Test method for resistance to short time hydraulic pressure of plastic pipe, tubing and fittings", ASTM D1599-99E01
8. "Test methods for sealability of gasket materials", ASTM F 37
9. "AWWA standard for GFR pressure pipe", ANSI AWWA C950-81, First Edition
10. " Standard for the design and performance of GRP pipes, and fittings for process plants", BS 6464
11. "Specification for glass reinforced plastics pipes, joints and fitting for use for water supply or sewerage", BS 5480
12. "Code of practice for design and construction of glass-reinforced plastics piping systems for individual plants or sites", BS 7159
13. "Glass fibre reinforced polyester resin pipe fittings and joints assemblies – Requirements for testing of bushes, flanges and flanged laminated joints", DIN 16966-7
14. "Fibre reinforced plastic composites – determination of fatigue properties under cyclic loading ",ISO/FDIS 13003
15. "Plastics piping systems – glass reinforced thermosetting plastics pipes and fittings – test methods to prove the leaktightness of the wall under short-term internal pressure", ISO 7511

16. “Fibre reinforced plastic composites – Determination of fatigue properties under cyclic loading”, ISO 10350-2
17. “Plastics piping systems – Glass reinforced thermosetting plastics pipes – determination of time to failure under sustained internal pressure”, ISO/DIS 7509
18. “Glass reinforced thermosetting plastic pipes and fittings – test methods to prove the design of bolted flange joints”, ISO/DIS 8483
19. “Plastics piping systems – glass reinforced thermosetting plastics pipes and fittings – methods for regression analysis and their use”, ISO 10928

APPENDIX B - MATERIAL PROPERTIES AND CURING GUIDELINE FOR NCS 993 PA RESIN

The material properties and the curing guideline of the NCS 993 PA resin provided by the supplier are listed below.

Table B.1: Properties of Cured NCS 993 PA (unfilled casting)

Temperature of deflection-under load (1,80MPa), °C	89
Water absorption, mg	35
Barcol (GYZJ 934-1) hardness	40
Elongation at break, % (void-free casting)	2.45
Tensile strength, MPa	76
Tensile modulus, MPa	3750
Volume shrinkage, %	7
Specific gravity @ 25°C, ratio	1.15

Table B.2: Conditioning guideline of the NCS 993 PA resin

100 Part NCS 993 PA catalysed with 2 phr BUTANOX M50	**Gel Time**
Geltime @ 15 °C, minutes	16
Geltime @ 25 °C, minutes	9
Geltime @ 35 °C, minutes	5

APPENDIX C - DESIGN OF STOPPERS

Steel stoppers were designed to avoid two major effects, namely, excessive deformation and failure by fracture. A finite element analysis using MSC Patran/Nastran software was conducted to estimate the stresses and deformation experienced by the stoppers at different loading conditions. The stress magnitudes predicted at different pressures were used to optimize the design of stoppers. Stoppers were made thick enough to minimize the deflection between two successive bolt holes. This is because an excessive bending effect could detrimentally affect the leak tightness of the joint. Adequate safety factors have been used since the consequences of failure by fracture of stoppers was not allowed. Two different types of stoppers have been designed and fabricated: The 10 bar and 20 bar stoppers (Figure C.1).

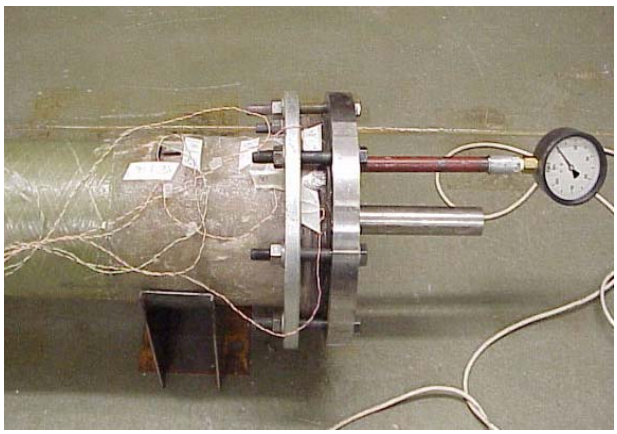


Figure C.1: Steel stopper sealing a 10 bar fabricated pipe flange

For design purposes of the stoppers, the term "safety factor" denotes the ratio of the strength of the material to the maximum computed stress when the system is loaded at 10.00 MPa [8]. In equation form, the safety factor is written as follows:

$$FS = \frac{Failure\ stress}{Maximum\ computed\ stress} \qquad \text{(Eq. C.1)}$$

Finite element analysis of stoppers

Stoppers were modelled and meshed as a 3D isotropic model. A distributed pressure load of 10.00 MPa was applied to the stoppers to simulate the pressure load generated by the maximum test pressure. Bolt holes were constraint for translation and rotation to simulate the clamping load generated by fasteners. The elastic modulus and the Poisson's ratio assigned to the material were 207 GPa and 0.32 respectively. A linear analysis was applied to the model. A sensitivity stress analysis was performed to improve the accuracy of the analytical results. The maximum stress results are listed in table C.1 while the predicted Von Mises stress-tensor and strain magnitude plots are presented in figure C.2 and C.3.

Table C.1: FEA results of stoppers

Stoppers	Maximum stress (MPa)
10 bar stopper	152
20 bar stopper	124

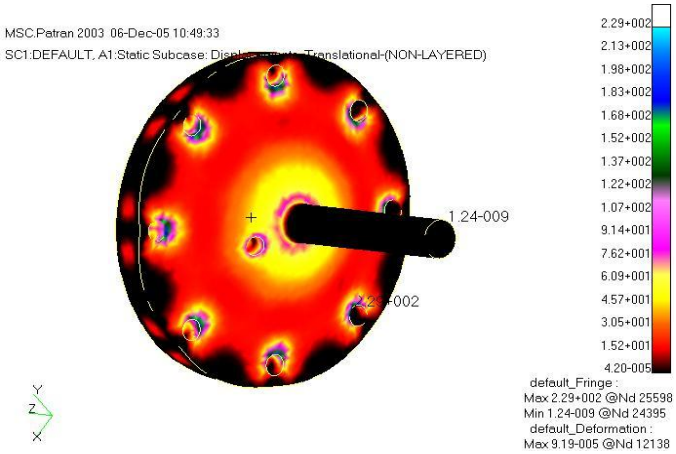


Figure C.2: Predicted Von Mises stresses for the 10 bar stopper

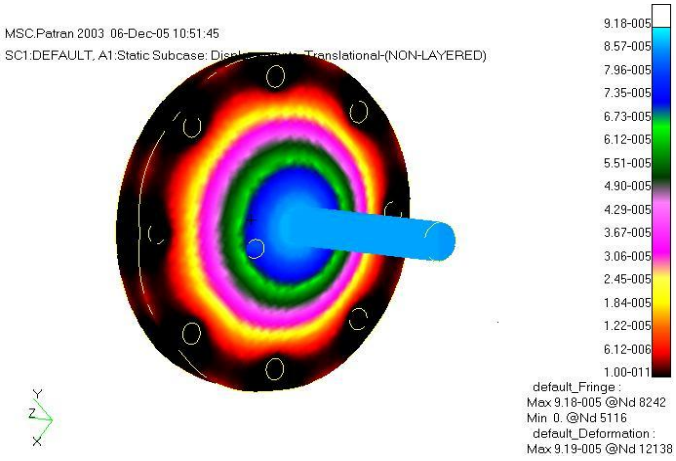


Figure C.3: Predicted strain magnitude for the 10 bar stopper

Calculation of Safety Factor

The estimated safety factors by yielding and fracture listed in table C.2 were determined by considering Eq. C.2 and Eq. C.3 respectively. These two equations derive from Eq. C.1. In Eq. C.2, the failure stress of the stopper denotes the material ultimate strength in tension (340 MPa) whereas in Eq. C.3 it denotes the material elastic strength in tension (220 MPa) [18]. Therefore, one can write:

$$\text{Safety factor by fracture} \qquad FS = \frac{Ultimate\ \ Strength}{Maximum\ computed\ \ stress} \qquad \text{(Eq. C.2)}$$

$$\text{Safety fracture by yielding} \qquad FS = \frac{Elastic\ \ Strength}{Maximum\ computed\ \ stress} \qquad \text{(Eq. C.3)}$$

Table C.2 Estimated safety factor of the 10 and 20 bar stoppers

Specimens	Safety factor by yielding	Safety factor by fracture
10 bar stopper	1.45	2.23
20 bar stopper	1.78	2.74

Figure C.1 and C.2 show that the maximum stress is around the bolt holes. The maximum strain is at the centre of the stopper. The holes intended to hold the pressure gauge and the pipe connector do not induce detrimental stress concentrations. At the seating conditions, the deformation between two successive bolt holes (0.00125 mm) was found to be smaller than the thickness of the compressed gasket (4.00 mm). Therefore, it was assumed that the seating pressure was evenly distributed.

APPENDIX D - DETERMINATION OF THE ESTIMATED INITIAL BOLT LOAD, END LOAD AND CLAMPING LOAD

Calculation of the estimated bolt loads at the initial tightening

The procedure presented below was followed to estimate the axial load experienced by bolts at the initial tightening and at different test pressures. M20 Class 8.8 steel bolts were used. To simplify the bolt analysis, the following assumptions were made:

- only the tensile stress was acting through the bolt shank
- linear elastic behaviour was obeyed.

The bolt torque magnitudes applied to the different joint assemblies were selected according to the BS 7159:1989 and BS 6464.

The following formula was used to calculate the estimated bolt load at the initial tightening [8] .

$$T=0.2\,DL \qquad \text{(Eq. D.1)}$$

Where T = initial bolt torque selected accordingly to BS 7159
D = nominal diameter of bolts (m)
L = initial bolt load (N)

Calculation of the axial bolt load and end load at different test pressures

At the initial tightening, the bolt load was calculated following the procedure presented above.

As the system is pressurized, the hydrostatic load acting axially on the stopper generates the axial load that tends to separate the flange and the stopper.
This load is expressed as

$$F = P\,\Pi\,R^2 \qquad \text{(Eq. D.2)}$$

Where P = actual test pressure applied to the joint system

R = internal radius of the flange

π = 3.142

Assuming that the reaction force that balances the load F is evenly distributed through each bolt, one can write

$$n\,L_b = P\;S \qquad \text{(Eq. D.3)}$$

Dividing Eq. D.3 by the number of bolts n, one obtains the axial bolt load L_b generated by the pressure test. Hence, the total axial load supported by each bolt at a given test pressure is calculated by summing up the axial load generated by the internal pressure and the initial bolt load.

$$L_t = L_b + L \qquad \text{(Eq. D.4)}$$

Note: L is the initial load of each bolt calculated above (Eq. D.4).

In order to calculate the longitudinal stress σ (end load) acting axially, the axial equilibrium state of the system was considered. This requires

$$P\,S = \sigma\,(2\,\pi\,R\,t) \qquad \text{(Eq. D.5)}$$

Solving for σ, one obtains

$$\sigma = \frac{P\,S}{(2\,\pi\,R\,t)}$$

Where t = thickness of the pipe wall

The clamping load experienced by the flange was calculated by dividing the resultant axial bolt load by the annular area of the contact surface between the backing ring and stub.

Table 10.4 Flange and bolt details for flanges to BS 1560 Class 150 dimensions 1½" to 24"

Stub flange						Backing flange							Bolt torque	
Root radii $R' \geq 3$ mm			Thickness (N)					Thickness (t')	Drilling					
			Strain class*	Pressure bar									Pressure bar	
			1 and 2	6	10			Pressure bar					6	10
Nominal size	Inside diameter (D_1)	Stub OD (D')	3	3	8	ID† (h)	OD (H)	10	Bolt size (inch)	No. of bolts	Hole size	p.c.d.		
			4	2	6									
	mm	mm		mm	mm	mm	mm	mm			mm	mm	N·m	N·m
40	40	135‡			10	67	135	10	0.5	4	15.9	98		25
50	50	102			10	78	152	10	0.625	4	19.0	121		20
80	80	133			11	112	190	10	0.625	4	19.0	152		25
100	100	172			15	142	229	12	0.625	8	19.0	191		20
150	150	219			17	186	279	13	0.75	8	22.2	241		35
200	200	276			20	237	343	15	0.75	8	22.2	298		45
250	250	337			24	298	406	18	0.875	12	25.4	362		55
300	300	406			29	365	483	21	0.875	12	25.4	432		75
350	350	448		25	29	423	533	22	1.00	12	28.6	476	70	95
400	400	511		29	32	467	597	24	1.00	16	28.6	540	70	95
450	450	546		27	30	508	635	25	1.125	16	31.8	578	75	115
500	500	603		30	34	564	698	27	1.125	20	31.8	635	70	115
550‡	550	648		32	36	614	756	30	1.125	20	31.8	692	80	120
600	600	714		34	38	669	813	32	1.25	20	34.9	749	100	170

*See table 4.3.
†ID of outer edge of chamfer is 6 mm greater.
‡Non-standard.
NOTE. See figure 10.2 for definitions of reference letters.

Figure D-1: Characteristics of flange and bolts [3]

APPENDIX E - PREDICTION OF THEORETICAL MATERIAL PROPERTIES

Introduction

The theoretical analysis based on the strength of materials approach, namely Micromechanics theory is one the methods extensively used in the prediction of the material properties of a flat and thin laminate. This approach is based on the micromechanics analysis of a unidirectional lamina. Taking into account some limitations, this concept yields accurate results when it is applied to other structures such as shells and beams [21].

Micro and Macromechanics of a unidirectional laminate

Being the starting point of a laminate analysis, the theoretical approach used to calculate the engineering constants of a continuous unidirectional fibre reinforced plastic requires some restrictions and assumptions that are listed bellow.

- perfect bonding exists between fibres and matrix
- both fibres and matrix are isotropic and obey Hooke's law
- fibres are continuous and parallel
- different layers of the structure are perfectly bonded together
- each layer has uniform thickness
- laminates are initially free of voids and cracks and are in a stress free state

Taking into account the rule of mixtures, the four engineering constants of the unidirectional lamina can be expressed in terms the elastic properties and volume fractions of different constituents as follows [19]:

$E1 = Ef^{*}\ Vf + Em^{*}Vm$ Longitudinal elastic modulus

$$E2 = \frac{Ef\ Em}{EfVm + EmVf}$$ Transverse elastic modulus

$v12 = vfVf + vmVm$ Major Poisson's Ratio

$$G12 = \frac{Gf\ Gm}{GfVm + GmVf}$$ Shear modulus of the lamina

$$Gf = \frac{Ef}{2(1 + Vf)}$$ Shear modulus of the fibre

$$Gm = \frac{Em}{2(1 + vm)}$$ Shear modulus of the matrix

$$v21 = v12 \quad \frac{E2}{E1}$$ Minor Poisson's Ratio

Where Ef = modulus of the fibre

Em = modulus of the matrix

vf = Poisson's ratio of the fibre

vm = Poisson's ratio of the fibre

Vf = fibre volume ratio

The fibre volume fraction is determined using the following equation

$$V_f = \frac{Wf / \rho f}{Wf / \rho f + (1 - Wf) / \rho m}$$

Where Wf is the experimental fibre content within the laminate

ρf and ρm are fibre and matrix specific gravity respectively

Assuming that the laminate is free of voids, the matrix volume ratio is determined using the following equation

$$Vm = Vf\text{-}1$$

Generally, the resulting force and moment in terms of the midplane strains and curvatures of a laminate are expressed in matrix form as [19].

$$\begin{bmatrix} Nx \\ Ny \\ Nxy \end{bmatrix} = \begin{bmatrix} A11 & A12 & A16 \\ A12 & A22 & A26 \\ A16 & A26 & A66 \end{bmatrix} \begin{bmatrix} \varepsilon x \\ \varepsilon y \\ \varepsilon xy \end{bmatrix} + \begin{bmatrix} B11 & B12 & B16 \\ B12 & B22 & B26 \\ B16 & B26 & B66 \end{bmatrix} \begin{bmatrix} \kappa x \\ \kappa y \\ \kappa xy \end{bmatrix} \quad \text{Eq. E.1}$$

$$\begin{bmatrix} Mx \\ My \\ Mxy \end{bmatrix} = \begin{bmatrix} B11 & B12 & B16 \\ B12 & B22 & B26 \\ B16 & B26 & B66 \end{bmatrix} \begin{bmatrix} \varepsilon x \\ \varepsilon y \\ \varepsilon xy \end{bmatrix} + \begin{bmatrix} D11 & D12 & D16 \\ D12 & D22 & D26 \\ D16 & D26 & D66 \end{bmatrix} \begin{bmatrix} \kappa x \\ \kappa y \\ \kappa xy \end{bmatrix} \quad \text{Eq. E.2}$$

Where

$$\text{Aij} = \sum_{k=1}^{n} \left[\overline{Qij}\right]_k \left(h_k - h_{k-1}\right) \quad \text{i} = 1,2,3;\ \text{j} = 1,2,3 \qquad \text{Eq. E.3}$$

Extensional stiffness matrix that relates the resultant in-plane forces to the in-plane strains:

$$Bij = \sum_{k=1}^{n} \left[\overline{Qij}\right]_k \left(h^2{}_k - h^2{}_{k-1}\right) \quad i = 1,2,3;\ j = 1,2,3 \qquad \text{Eq. E.4}$$

Extension-bending coupling matrix that couples the force and moment terms to the midplane strains and midplane curvatures:

$$Dij = \sum_{k=1}^{n} \left[\overline{Qij}\right]_k \left(h^3{}_k - h^3{}_{k-1}\right) \qquad i = 1,2,3;\ j = 1,2,3 \qquad \text{Eq. E.5}$$

Where $[Qij]$ = Reduced stiffness matrix

$\left[\overline{Qij}\right]$ = Transformed reduced stiffness matrix

h_k = Coordinate location of the k-th layer

h = Thickness of the lamina

n = Number of lamina in the structure

The thickness of the laminate is determined using the formula:

$$h = n\left(\frac{mf + m_m}{\rho f + \rho m}\right)$$

Where mf and m_m are the aerial masses of the fibre and matrix respectively

Assuming that all laminae (CSM and WR) have practically the same thickness, the extensional stiffness matrix, extension-bending coupling matrix and bending stiffness matrix can be expressed as:

$$Aij = \sum_{k=1}^{n} \left[\overline{Qij}\right]_k h$$

$$Bij = \sum_{k=1}^{n} \left[\overline{Qij}\right]_k h\ \overline{Z_k}$$

$$Dij = \sum_{k=1}^{n} \left[\overline{Qij}\right]_k \left(h\overline{Z_k^a} + \frac{t_k^3}{12}\right)$$

Where $\overline{Z_k}$ stands for the distance of the mid-surface of the *k*-th layer lamina to the middle surface of the laminate. However, laminate thickness was determined experimentally.

Calculation of apparent elastic moduli and thermal strains

The theoretical prediction of the material properties for the flange wall and pipe wall is based on the Classical Lamination Theory, and was performed using a MATLAB computer code. Woven roving and chopped strand mat laminates were modelled as [0/90/±45]s and [0/90]s quasi-isotropic laminates respectively. The average experimental fibre volume fractions obtained from burn off tests were used to improve the model accuracy.

The reduced stiffness matrix *Qij* of each type of layer (CSM or WR) was determined using the four elastic moduli of the corresponding unidirectional lamina. The reduced stiffness matrix allowed determining the transformed reduced stiffness matrix of the lamina. Taking into account the packing sequence of the laminate, the transformed reduced stiffness matrix and the lamina coordinate (coordinate of the top and the bottom surface of each layer in terms of the mid-plane of the laminate) were used to calculate the extensional stiffness matrix A*ij* that allowed calculation of the laminate engineering constants.

The four apparent engineering constants of the flange wall and the pipe constructions were calculated using the equations listed below [19].

$$Ex = \left(A11 - \frac{A^2 12}{A22} \right) / n*h \qquad \text{In-plane longitudinal elastic modulus}$$

$$Ey = \left(A22 - \frac{A^2 12}{A11} \right) / n*h \qquad \text{In-plane transverse elastic modulus}$$

$$Gxy = \frac{A66}{n*h} \qquad \text{In-plane shear modulus}$$

$$vxy = \frac{A12}{A22} \qquad \text{Major Poisson's ratio}$$

$$vyx = \frac{A12}{A11} \qquad \text{Minor Poisson's ratio}$$

The through thickness *Ez* was assumed to be similar to that of the corresponding unidirectional lamina. The coefficient of thermal expansion of the CSM and WR plies were calculated using the following formula [19]:

$$\begin{bmatrix} \alpha x \\ \alpha y \\ \alpha xy \end{bmatrix}_{\substack{\Delta C=0 \\ \Delta T=1}} = \begin{bmatrix} A11 & A12 & A16 \\ A12 & A22 & A26 \\ A16 & A26 & A66 \end{bmatrix}^{-1} \begin{bmatrix} N_x^T \\ N_y^T \\ N_{xy}^T \end{bmatrix} \qquad \text{Eq. E.6}$$

Where $\begin{bmatrix} N_x^T \\ N_y^T \\ N_{xy}^T \end{bmatrix} = \Delta T \sum_{k=1}^{n} \left[\overline{Qij}\right]_k \begin{bmatrix} \alpha x \\ \alpha y \\ \alpha xy \end{bmatrix}_k$ Fictitious thermal load

$\begin{bmatrix} \alpha x \\ \alpha y \\ \alpha xy \end{bmatrix}_k$ Transformed CTE of the corresponding unidirectional lamina

ΔT and ΔC denoted the temperature change and the weight of moisture absorption per unit weight of the lamina. ΔC was not taken into account, since the testing time did not allow the swelling strains and stresses generated by the moisture change in the flange structure to be accounted for. The material properties of resin and E-glass fibre listed in table E.1 were used to predict the material properties of different lamina. The predicted material properties assigned to the Amitech flange models are listed in table E.2.

Table E.1: Material properties of Polyester resin and E-glass

Material	**Specific gravity**	**Young's modulus**	**Tensile Strength**	**Tensile elongation**	**CTE**
		(GPa)	(GPa)	(%)	m/m/°C
E-Glass	2.60	72.00	1.72	2.40	5.58
Polyester resin NCS 993 PA	1.15	3.75	0.076	2.45	70.00

Table E.2: Predicted material properties assigned to Amitech flange models

Material Properties of lamina	CSM lamina	WR lamina	Fibre wound Pipe construction
Ex (Gpa)	8.17	13.86	6.93
Ey (Gpa)	8.17	13.86	13.84
Ez (Gpa)	4.13	4.12	4.13
*Gx*y (Gpa)	3.10	1.90	9.42
vxy	0.32	0.11	0.42
Vxz, vyz	0.38	0.37	0.83
αx (με)	35.33	24.47	16.3
αy (με)	35.33	24.47	6.95
Glass content (%)	32	45	68

APPENDIX F - EXPERIMENTAL COEFFICIENTS OF THERMAL EXPANSION

Axial and circumferential coefficients of thermal expansion determined experimentally are listed below. The procedure followed to perform the calibration is described in section 3.5.

Table F.1: Experimental coefficients of thermal expansion

	Coefficient of Thermal Expansion α (με /°C)					
Amitech flanges	**Location 1**		**Location 2**		**Location 3**	
	Axial	**Hoop**	**Axial**	**Hoop**	**Axial**	**Hoop**
10 bar flange 1	20.50	9.92	32.20	11.50	18.56	9.96
10 bar flange 2	18.92	11.20	30.52	13.30	15.89	10.10
16 bar flange 1	22.80	10.41	35.40	12.45	23.10	11.02
16 bar flange 2	18.02	11.30	38.54	15.65	19.42	9.70
20 bar flange 1	22.40	10.51	32.61	16.45	20.00	10.10
20 bar flange 2	19.50	9.60	35.90	12.50	18.51	9.78
Fabricated flanges						
10 bar flange 1	32.12	30.27	35.10	36.20	18.12	10.20
10 bar flange 2	36.23	32.01	31.20	29.90	16.50	8.56

APPENDIX G - COMPARISON OF EXPERIMENTAL STRAINS AT LOCATION 2 BETWEEN AMITECH SPECIMENS

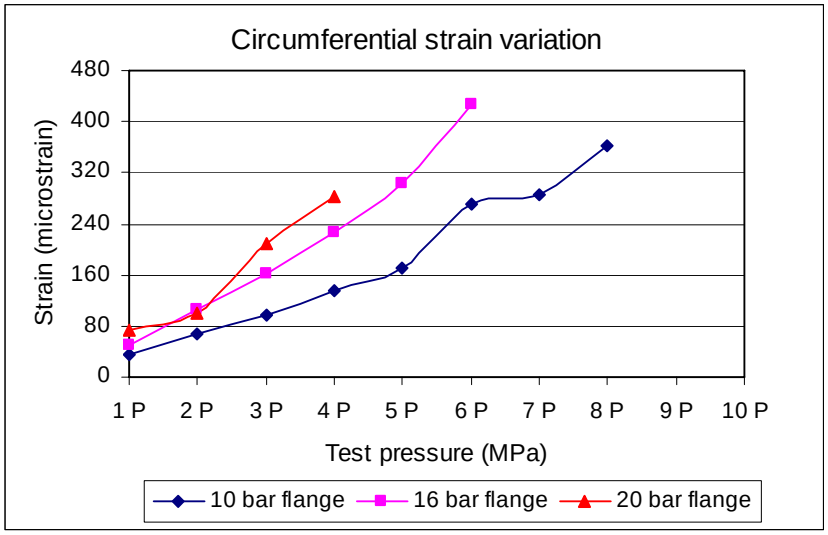


Figure G.1: Circumferential strains of flange 1

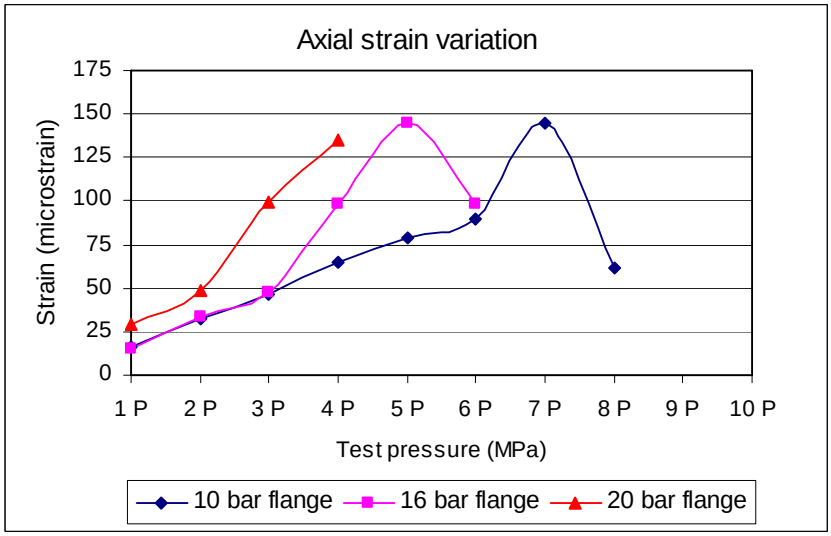


Figure G.2: Axial strains of flange 1

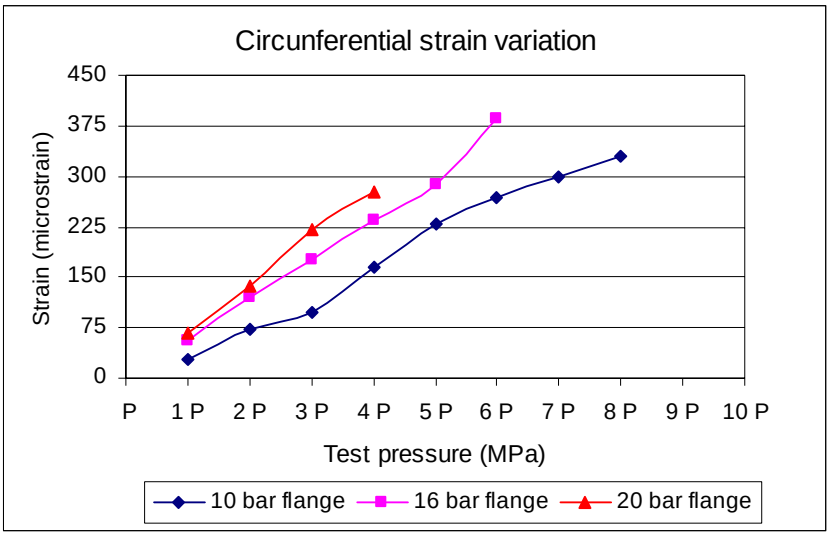


Figure G.3: Circumferential strains of flange 2

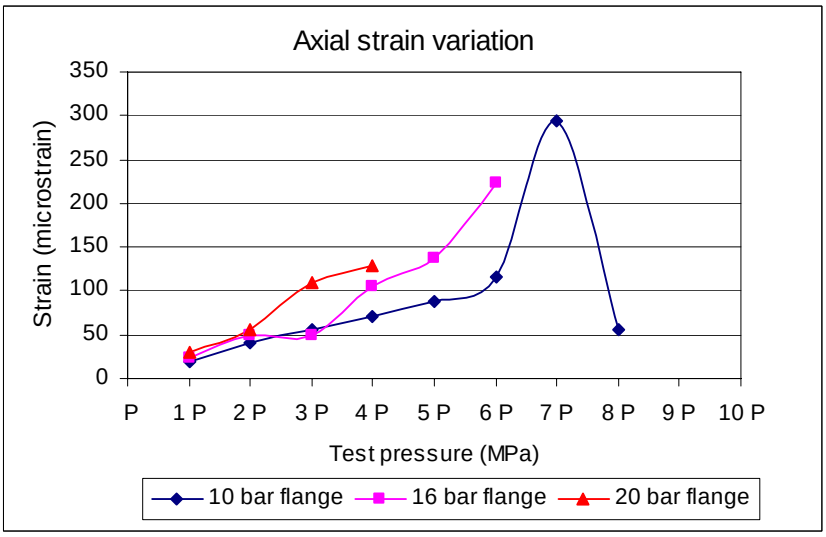


Figure G.4: Axial strains of flange 2

APPENDIX H - COMPARISON OF EXPERIMENTAL STRAINS AT LOCATION 1 BETWEEN AMITECH SPECIMENS

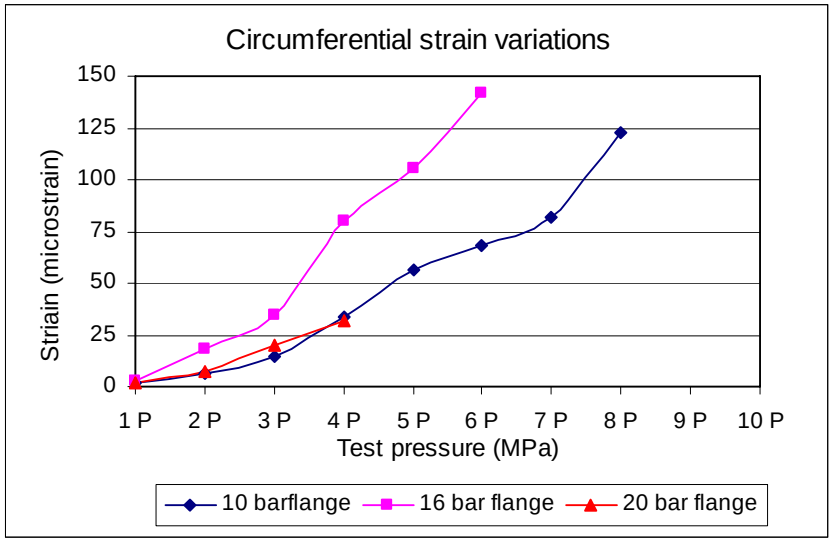


Figure H.1: Circumferential strains of flange 1

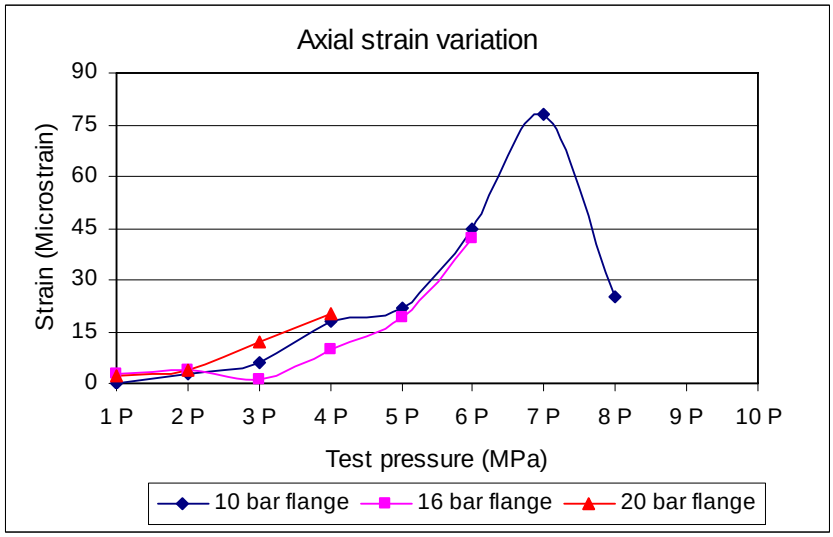


Figure H.2: Axial strains of flange 1

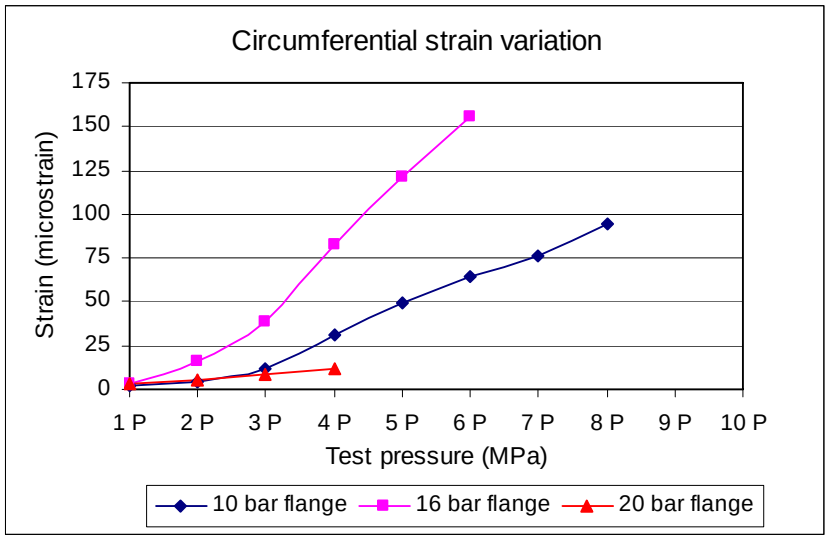


Figure H.3: Circumferential strains of flange 2

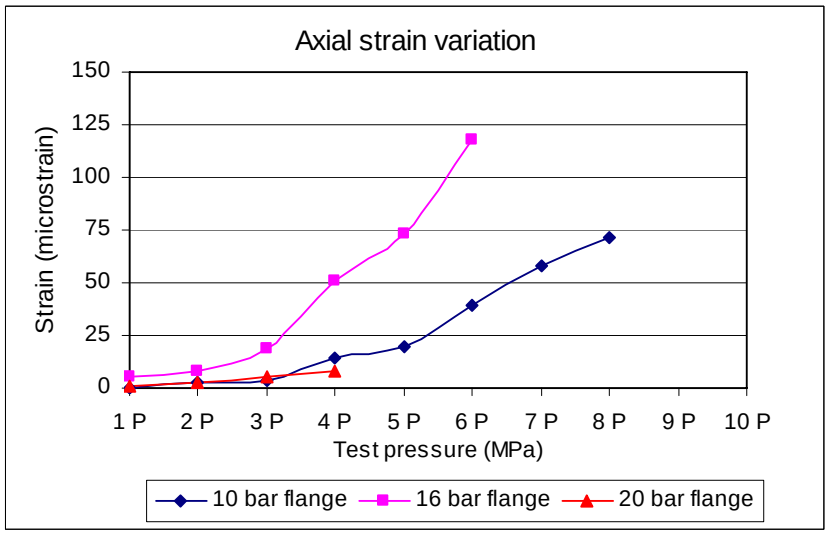


Figure H.4: Axial strains of flange 2